On the Mechanism of *cis*-Dihydroxylation and Epoxidation of Alkenes by highly H_2O_2 efficient Dinuclear Manganese Catalysts.

Johannes W. de Boer,[a] *Wesley R. Browne,*[a] *Jelle Brinksma,*[a] *Paul L. Alsters,*[b] *Ronald Hage*[c] *and Ben L. Feringa*[a]*

Online Supporting information

Synthesis and physical data

$[Mn_2(\mu\text{-}O_2H_3)(\mu\text{-}CCl_3CO_2)_2(tmtacn)_2]PF_6$. (**2c**)

Hydrazine.hydrate (20 μL, 0.2 mmol) was added to a solution of **1** (81 mg, 0.10 mmol) and trichloroacetic acid (35 mg, 0.22 mmol) in 20 ml of CH_3CN with stirring. The solution changed from red to light purple to colorless over 30 min. The solvent was evaporated to near dryness and the white precipitate washed with diethyl ether. Yield 88 % (84 mg, 0.088 mmol). Mass spec. (calc. $Mn_2C_{22}H_{45}N_6Cl_6O_6$ m/z) **2c**$^+$ 809.0 (809.0), isotope pattern in agreement predicted pattern for 6×Cl; Elemental analysis (calc. $Mn_2C_{22}H_{45}N_6Cl_6O_6PF_6$) C 26.5% (27.6%), H 4.23% (4.74%), N 8.79 % (8.78%).

$[Mn_2(\mu\text{-}O)(\mu\text{-}O_2C(CH_2)_3CO_2)_2(tmtacn)_2](PF_6)_2$. (**4**)

L-Ascorbic acid (19 mg, 0.105 mmol) in 2 ml of H_2O was added to a solution of **1** (81 mg, 0.10 mmol) and glutaric acid (14 mg, 0.106 mmol) in 20 ml of H_2O with rapid stirring. The red/purple precipitate was isolated by filtration and recrystallized from acetonitrile by slow diffusion of

diethylether. Yield 45 % (40 mg, 0.045 mmol). Mass spec. (calc. $Mn_2C_{23}H_{48}N_6O_5$ m/z) **4**$(PF_6)^+$ 743.5 (743.5), **4**$_2PF_6^{3+}$ 447.3 (447.3), **4**$^{2+}$ 299.4 (299.5); ^{1}H NMR (400 MHz, CD_3CN) δ 74, 70, 40, 19, 10, -76, -88, -102. Elemental analysis (calc. $Mn_2C_{23}H_{48}N_6O_5P_2F_{12}$) Mn 12.35 % (12.32 %), C 31.2 % (31.0 %), H 5.54 % (5.39 %), N 9.35 % (9.44 %).

[Mn_2(μ-O)(μ-2,4-dichlorobenzoate)$_2$(tmtacn)$_2$](PF_6)$_2$. (**6**)

As for **4** except 2,4-dichlorobenzoic acid (42 mg, 0.22 mmol) was employed. Yield 62 % (75 mg, 0.062 mmol). Mass spec. (calc. $Mn_2C_{32}H_{48}N_6Cl_4O_5$ m/z) **6**$(PF_6)^+$ 991.3 (991), **6**$^{2+}$ 424.3 (424), isotope pattern in agreement predicted pattern for 4×Cl; ^{1}H NMR (400 MHz, CD_3CN) δ 65, 42, 36, 15, -80, -93, -100. Elemental analysis (calc. $Mn_2C_{32}H_{48}N_6Cl_4O_5P_2F_{12}$) C 33.6 % (33.7 %), H 4.47% (4.22 %), N 7.51 % (7.38 %).

[Mn_2(μ-O)(μ-2,6-dichlorobenzoate)$_2$(tmtacn)$_2$](PF_6)$_2$. (**7**)

As for **4** except 2,6-dichlorobenzoic acid (42 mg, 0.22 mmol) was employed. Yield 40 % (50 mg, 0.044 mmol). Mass spec. (calc. $Mn_2C_{32}H_{48}N_6Cl_4O_5$ m/z) **7**$(PF_6)^+$ 991.3 (991), **7**$^{2+}$ 424 (424), isotope pattern in agreement predicted pattern for 4×Cl; ^{1}H NMR (400 MHz, CD_3CN) δ 65, 42, 36, 15, -80, -93, -100. Elemental analysis (calc. $Mn_2C_{32}H_{48}N_6Cl_4O_5P_2F_{12}$) C 33.6 % (33.7 %), H 4.27% (4.22 %), N 7.30 % (7.38 %).

[Mn_2(μ-O)(μ-2,4,6-trichlorobenzoate)$_2$(tmtacn)$_2$](PF_6)$_2$. (**10**)

As for **4** except 2,4,6-trichlorobenzoic acid (46 mg, 0.22 mmol) was employed. Yield 62 % (75 mg, 0.062 mmol). Mass spec. (calc. $Mn_2C_{32}H_{46}N_6Cl_6O_5$ m/z) **10**$(PF_6)^+$ 1059.0 (1059), **10**$^{2+}$ 457.3 (457), isotope pattern in agreement predicted pattern for 6×Cl; ^{1}H NMR (400 MHz, CD_3CN) δ 66, 35, 32, 15, -74, -87, -108. Elemental analysis (calc. $Mn_2C_{32}H_{46}N_6Cl_6O_5P_2F_{12}$) C 31.4 % (31.8 %), H 4.05% (3.81 %), N 7.08 % (6.96 %).

$[Mn_2(\mu\text{-}O)(\mu\text{-}3\text{-chlorobenzoate})_2(tmtacn)_2](PF_6)_2$. (**11**)

As for **4** except 3-chlorobenzoic acid (34 mg, 0.22 mmol) was employed. Yield 25 % (30 mg, 0.028 mmol). Mass spec. (calc. $Mn_2C_{32}H_{50}N_6Cl_2O_5$ m/z) **11**$(PF_6)^+$ 923.3 (923), **11**$^{2+}$ 389.3 (389), isotope pattern in agreement predicted pattern for 2×Cl; ^{1}H NMR (400 MHz, CD_3CN) δ 66, 35, 32, 15, -74, -87, -108. Elemental analysis (calc. $Mn_2C_{32}H_{50}N_6Cl_2O_5P_2F_{12}$) C 36.0 % (35.9 %), H 4.98% (4.68 %), N 7.80 % (7.86 %).

$[Mn_2(\mu\text{-}O)(\mu\text{-}4\text{-hydroxybenzoate})_2(tmtacn)_2](PF_6)_2$. (**9**)

As for **4** except 4-hydroxybenzoic acid (31 mg, 0.22 mmol) was employed. Yield 63 % (72 mg, 0.07 mmol). Mass spec. (calc. $Mn_2C_{32}H_{52}N_6O_7$ m/z) **9**$(PF_6)^+$ 887.3 (887), **9**$^{2+}$ 371.3 (371); ^{1}H NMR (400 MHz, CD_3CN) δ 72, 35, 19, 13.5, 8, -1, -80, -95. Elemental analysis (calc. $Mn_2C_{32}H_{52}N_6O_7P_2F_{12}$) C 34.5% (37.2%), H 5.18% (5.04 %), N 7.56 % (8.14%).

$[Mn_2(\mu\text{-}O)(\mu\text{-}2,4\text{-difluorobenzoate})_2(tmtacn)_2](PF_6)_2$. (**12**)

As for **4** except 2,4-difluorobenzoic acid (70 mg, 0.44 mmol) and **1** (162 mg, 0.20 mmol) was employed. Yield 47 % (100 mg, 0.093 mmol). Mass spec. (calc. $Mn_2C_{32}H_{48}N_6O_5F_4$ m/z) **12**$(PF_6)^+$ 927.3 (927), **12**$^{2+}$ 391.3 (391); ^{1}H NMR (400 MHz, CD_3CN) δ 66, 35, 32, 15, -74, -87, -108. ^{19}F NMR (121.5 MHz), -55, -84 ppm. Elemental analysis (calc. $Mn_2C_{32}H_{48}N_6O_5P_2F_{16}$) C 35.9 % (35.8%), H 4.39% (4.48 %), N 7.75 % (7.84 %).

$[Mn_2(\mu\text{-}O)(\mu\text{-}2,6\text{-difluorobenzoate})_2(tmtacn)_2](PF_6)_2$. (**13**)

As for **4** except 2,6-difluorobenzoic acid (35 mg, 0.22 mmol) was employed. Yield 72 % (85 mg, 0.079 mmol). Mass spec. (calc. $Mn_2C_{32}H_{48}N_6O_5F_4$ m/z) **13**$(PF_6)^+$ 927.3 (927), **13**$^{2+}$ 391.2 (391); ^{1}H NMR (400 MHz, CD_3CN) δ 70, 34, 19, 7, -79, -90, -100 ppm. ^{19}F NMR (121.5 MHz), -58 ppm. Elemental analysis (calc. $Mn_2C_{32}H_{48}N_6O_5P_2F_{16}$) C 37.3 % (35.8%), H 5.27 % (4.48 %), N 7.10 % (7.84 %).

$[Mn_2(\mu\text{-}O)(\mu\text{-}3,4\text{-difluorobenzoate})_2(tmtacn)_2](PF_6)_2$. (**14**)

As for **4** except 3,4-difluorobenzooic acid (35 mg, 0.22 mmol) was employed. Yield 63 % (75 mg, 0.07 mmol). Mass spec. (calc. $Mn_2C_{32}H_{48}N_6O_5F_4$ m/z) **14**$(PF_6)^+$ 927.3 (927), **14**$^{2+}$ 391.2 (391); ^{1}H NMR (400 MHz, CD_3CN) δ 70, 34, 19, 14.5, 13, 7, -79, -90, -98 ppm. ^{19}F NMR (121.5 MHz), -127.5, -104.5 ppm. Elemental analysis (calc. $Mn_2C_{32}H_{48}N_6O_5P_2F_{16}$) C 36.3 % (35.8%), H 5.35% (4.48 %), N 7.50 % (7.84 %).

$[Mn_2(\mu\text{-}O)(\mu\text{-}3,5\text{-difluorobenzoate})_2(tmtacn)_2](PF_6)_2$. (**15**)

As for **4** except 3,5-difluorobenzoic acid (70 mg, 0.44 mmol) and **1** (162 mg, 0.20 mmol) were employed. Yield 60 % (125 mg, 0.12 mmol). Mass spec. (calc. $Mn_2C_{32}H_{48}N_6O_5F_4$ m/z) **15**$(PF_6)^+$ 927.3 (927), **15**$^{2+}$ 390.6 (391); ^{1}H NMR (400 MHz, CD_3CN) δ 70, 35, 34, 18, 7.5, 5.5, -79, -90, -96 ppm. ^{19}F NMR (121.5 MHz), -99 ppm. Elemental analysis (calc. $Mn_2C_{32}H_{48}N_6O_5P_2F_{16}$) C 36.0 % (35.8 %), H 4.52% (4.48 %), N 7.95 % (7.84 %).

$[Mn(2\text{-oxybenzoate})(tmtacn)](PF_6)$. (**8**)

2-hydroxybenzoic acid (16 mg, 0.116 mmol) is added to **3** (50 mg, 0.058 mmol) in 20 mL of CH_3CN. The solution is evaporated and precipitate dissolved in a further 20 mL of CH_3CN and $^iPr_2O$ (10 mL) were added. The green crystals were washed with diethyl ether and air dried. Yield 91 % (54 mg, 0.106 mmol). Mass spec. (calc. m/z) (**8**$^+$) 361.9 (362), (calc. 8$^+$ + CH_3CN m/z) **8**$^+$ 403 (403); ^{1}H NMR (400 MHz, CD_3CN) δ –12, -20, -30 ppm. Elemental analysis (calc. $MnC_{16}H_{26}N_3O_3PF_6$) Mn 10.72 (10.85 %), C 37.7 % (37.8%), H 5.23% (4.93%), N 8.22 % (8.28%).

Table S1 Redox data for $[Mn_2(\mu\text{-}O)(\mu\text{-}RCO_2)_2(tmtacn)_2]^{n+}$ complexes in CH_3CN/0.1 M $TBAPF_6$

	R	$E_{1/2}^{II/III\text{-}III/III}$	$E_{1/2}^{III/III\text{-}III/IV}$	$E_{1/2}^{III/IV\text{-}IV/IV}$
2a	CCl_3	0.25 (79)	1.40 (130)	2.06 ($E_{p,a}$, irr)
3	CH_3	-0.28	0.985	1.61
4	$-(CH_2)_3$	-0.25 ($E_{p,c}$)	1.05 (156)	1.73 (230)
7	2,6-dichlorobenzoate	0.075 (70)	1.24 (102)	1.85 (130)
6	2,4-dichlorobenzoate	0.005 (76)	1.16 (100)	1.775 (130)
9	4-hydroxybenzoate	-0.08 ($E_{p,c}$, irr)	1.01 (130)	1.56 ($E_{p,a}$, irr)
10	2,4,6-trichlorobenzoate	0.08 (110)	1.25 (170)	1.86 (120)
11	3-chlorobenzoate	0.02 (70)	1.15 (110)	1.70 (150)
12	2,4-difluorobenzoate	-0.02 (75)	1.11 (90)	1.68 (120)
13	2,6-difluorobenzoate	0.01 (90)	1.16 (130)	1.72 (100)
14	3,4-difluorobenzoate	0.00 (60)	1.11 (80)	1.69 (120)
15	3,5-difluorobenzoate	0.01 (77)	1.15 (120)	1.71 (110)

Catalytic oxidation of cyclooctene.

Table S2 **1** and $[Mn_2(\mu\text{-}O)(\mu\text{-}RCO_2)_2(tmtacn)_2]^{2+}$ complexes – lag-time and effect of pretreatment on the catalytic oxidation of cyclooctene

Entry	**catalyst**	**Acid (mol%)**	**conv.**	**t.o.n.**		**mass.**	**remarks**
	(mol%)		**(%)**	***cis*-diol**	**epoxide**	**bal. (%)**	
I	**1**	trichloroacetic (1)	82	445	227	85	pretreatment H_2O_2
II	**2a**	trichloroacetic (1)	93	380	259	71	
III	**2a**	-	44	269	112	94	
IV	**3**	acetic (1)	29	210	88	101	
V	**3**	trichloroacetic (1)	91	378	247	72	
VI	**1**	2,6-dichlorobenzoic (1)	36	326	21	98	1.3 equiv H_2O_2
VII	**1**	2,6-dichlorobenzoic (1)	44	395	36	99	pretreat. H_2O_2, 1.3 equiv H_2O_2,
VIII	**1**	2,6-dichlorobenzoic (3)	70	525	75	93	pretreat. H_2O_2, 1.8 equiv H_2O_2
IX	**7**	2,6-dichlorobenzoic (3)	62	494	62	94	
X	**1**	2,3,6-trichlorobenzoic (1)	39	358	30	99	1.3 equiv H_2O_2
XI	**1**	2,3,6-trichlorobenzoic (1)	42	362	30	97	1.3 equiv H_2O_2
XII	**1**	2,3,6-trichlorobenzoic (3)	61	505	57	95	1.3 equiv H_2O_2
XIII	**1**	2,3,6-trichlorobenzoic (3)	54	424	61	94	r.t.; 1.3 equiv H_2O_2
XIV	**1**	2,4,6-trichlorobenzoic (1)	24	197	16	97	
XV	**10**	2,4,6-trichlorobenzoic (1)	26	253	24	102	
XVI	**10**	2,4,6-trichlorobenzoic (1)	37	292	26	95	H_2O-pretreatment
XVII	**1**	2-hydroxybenzoic acid (1)	64	225	320	90	
XVIII	**8**	2-hydroxybenzoic acid (1)	75	249	371	87	

Table S3 Effect of relative acid concentration on the product distribution following catalytic oxidation of cyclooctene with H_2O_2 catalyzed by **1**.[a]

Entry No.	**additive (mol%)**	**conv. (%)**	**t.o.n.**		**mass. bal. (%)**
			***cis*-diol**	**epoxide**	
I	trichloroacetic (0.1)[b]	9	63	27	100
II	trichloroacetic (0.2)[b]	59	341	144	90
III	trichloroacetic (0.4)	65	349	165	86
IV	trichloroacetic (1)[b]	91	438	247	78
V	trichloroacetic (1)[c]	91	380	280	75
VI	trichloroacetic (25)[b]	96	324	406	77
VII	trichloroacetic (25)[d]	94	432	285	77
VIII	acetic (1)	14	78	36	98
IX	acetic (25)	67	307	303	94
X	2,6-dichlorobenzoic (1)	36	320	21	98
XI	2,6-dichlorobenzoic (1)[e]	44	395	36	99
XII	2,6-dichlorobenzoic (1)[c]	48	357	44	93
XIII	2,6-dichlorobenzoic (3)[e]	67	525	75	93
XIV	salicylic (1)	64	225	320	90
XV	salicylic (5)	74	132	510	90
XVI	salicylic (10)	61	102	431	92
XVII	trifluoroacetic (25)	92	322	389	79
XVIII	trifluoroacetic (1)	90	296	251	65

a) 0.1 mol% catalyst in CH_3CN at 0 ^oC b) from ref 1 c) at 20 ^oC d) in CH_3CN/H_2O 9:1. e) pre-treatment of **1**/carboxylic acid with 30 µL H_2O_2 at 20 ^oC 20 min prior to cooling to 0 ^oC and addition of cyclooctene.

Table S4 Product distribution following catalytic oxidation of cyclooctene with **1, 2a, 2b** and **2c** (0.1 mol%) at 0 ^{o}C in the presence of trichloroacetic (1 mol%) with and without prior addition of H_2O (see text for details).

Entry	catalyst	Vol. H_2O[a]	conv. (%)	t.o.n.		mass. bal. (%)
				cis-diol	epoxide	
I	**1**	-	91	438	247	78
II	**2a**	-	93	380	259	71
III	**2a**	110 µL	96	357	250	65
IV	**2b**		90	378	280	76
V	**2b**	110 µL	93	390	251	71
VI	**2b**[b]	-	76	403	217	86
VII	**2c**	-	91	372	252	71

a) added prior to addition of cyclooctene and H_2O_2 b) 30 µL of H_2O_2 added at 20 ^{o}C prior to addition of cyclooctene

Table S5 Product distribution following catalytic oxidation of cyclooctene by **2a** (0.1 mol%) at 0 ^{o}C in the presence of trichloroacetic (1 mol%) using dried H_2O_2 (0.46 eqv.) with and without addition of extra H_2O (see text for details).

Entry	catalyst (mol%)	Extra water	conv.	t.o.n.		mass.
			(%)	*cis*-diol	epoxide	bal. (%)
I	**2a**	dry	29	151	102	96
II	**2a**	'wet'	38	254	104	96

Table S6 Solvent dependence on the product distribution following oxidation of cyclooctene catalyzed by **1**, **2a** or Mn(II)SO_4 with CCl_3CO_2H (1 mol%).

Entry	catalyst (mol%)	solvent	conv.	t.o.n.		mass.
			(%)	*cis*-diol	epoxide	bal. (%)
I	**1** (0.1)	CH_3CN	91	438	247	78
II	**1** (0.1)	$^tBuOH/H_2O$(2:1 v/v)	39	227	90	93
III	**1** (0.1)	THF	21	115	43	95
IV	**2a** (0.1)	THF	23	106	64	94
V	**1** (0.1)	Acetone	53	176	138	78
VI	**2a** (0.1)	Acetone	63	205	183	75
VII	**1** (0.1)	DMF[b]	20	0	7	80
VIII	$MnSO_4$ (1)[a]	DMF[b]	3	0	5	98
IX	**1** (0.1)	CH_2Cl_2	15	20	70	94

a) 10 mol% CCl_3CO_2H b) Both spectroscopic grade and 'amine free' peptide synthesis grade DMF were tested. Complex **2a** was found to be very unstable in DMF (with a rapid loss of the characteristic UV.Vis spectrum of **2a**), even in the absence of H_2O_2 and the conversion of **1** to **2a** was not observed. In dichloromethane, reaction of **1**/CCl_3CO_2H with dihydrogen peroxide was observed, however, the stability of **2a** was found to be poor (by UV.Vis spectroscopy).

Table S7 Product distribution following oxidation of cyclooctene catalyzed by **2a** (0.1 mol%) at 0 ^oC in the presence of trichloroacetic (1.0 mol%) with H_2O_2 and D_2O_2.

Entry	Oxidant[a]	conv.	t.o.n.		mass.
		(%)	*cis*-diol	epoxide	bal. (%)
I	30% H_2O_2 [b]	89	423	238	77
II	30% H_2O_2 (diluted from 50% with H_2O)	92	403	241	73
III	30% H_2O_2 (diluted from 50% with D_2O)	90	415	240	75
IV	30% D_2O_2 (in D_2O)[b]	94	394	248	70

a) reactions were performed in 15 ml instead of 10 mL of CH_3CN to prevent phase separation of the CH_3CN and cyclooctene. b) used as received without dilution

Table S8 *Cis*-dihydroxylation and epoxidation of cyclooctene (including mass-balance) – influence of carboxylic acid[a]

entry	Catalyst	Co-catalyst (mol%)	conv.%[b]	T.O.N.[c]		Mass	Lag-period (h)
				cis-diol	epoxide	Bal. (%)	
I	**1**	Acetic acid (1.0)	14	78	36	98	>1.5 h
II	**1**	glutaric (0.5)	38	237	104	96	2-3 h
III	**1**	CCl_3CO_2H (1.0)[b]	91	440	245	78	60-90 min
IV	**1**	Trifluoroacetic (1.0)	90	296	251	65	30-45 min
V	**1**	hexafluoroglutaric (0.5)	92	315	256	65	15-30 min
VI	**1**	Benzoic acid (1.0)	21	110	60	96	>2h
VII	**1**	2-chlorobenzoic acid (1.0)	29	165	80	96	>2h
VIII	**1**	3-chlorobenzoic acid (1.0)	38	253	113	98	N/A
IX	**1**	4-chlorobenzoic acid (1.0)	16	88	42	97	>2h
X	**1**	2,6-dichlorobenzoic acid (1.0)	36	320	21	98	1.5 h
XI	**1**	2,4-dichlorobenzoic acid (1.0)	21	128	47	97	>2h
XII	**1**	2,3,6-trichlorobenzoic acid (1.0)	42	362	30	97	1.25 h
XIII	**1**	2,4,6-trichlorobenzoic acid (1.0)	24	197	16	97	2-3 h
XIV	**1**	2,4,6-trimethylbenzoic acid (1.0)	7	40	8	98	>2h
XV	**13**	2,6-difluorobenzoic acid (1.0)	47	301	103	93	1.5 h
XVI	**12**	2,4-difluorobenzoic acid (1.0)	43	268	106	95	2 h
XVII	**14**	3,4-difluorobenzoic acid (1.0)	34	206	82	95	2 h
XVIII	**1**	3,5-difluorobenzoic acid (1.0)	20	101	51	95	1 h
XIX	**15**	3,5-difluorobenzoic acid (0.0)	10	50	23	97	3 h
XX	**15**	3,5-difluorobenzoic acid (1.0)	33	194	82	95	1.25 h
XXI	**1**	2-methoxybenzoic acid (1.0)	47	244	158	93	2 h
XXII	**1**	4-methoxybenzoic acid (1.0)	26	137	83	96	>2h
XXIII	**1**	2-hydroxybenzoic acid (1.0)	64	225	320	90	1.25 h
XXIV	**1**	3-hydroxybenzoic acid (1.0)	69	260	325	89	1.5 h
XXV	**1**	4-hydroxybenzoic acid (1.0)	46	219	170	93	>2 h
XXVI	**1**	5-bromo2-hydroxybenzoic acid (1.0)	62	252	296	92	N/A

[a] **1** (0.1 mol%). [b] Data from ref. 1.

Table S9 $^{16/18}O$ isotopic distribution in the oxidation products of cyclooctene by $[Mn^{III}_2(\mu\text{-}O)(\mu\text{-carboxylato})_2(tmtacn)_2]^{2+}$ complexes (0.1 mol%) at 0 °C in the presence of the corresponding carboxylic acid with $H_2{}^{18}O_2/H_2{}^{16}O$ and $H_2{}^{16}O_2/H_2{}^{18}O$. Product isotope distribution was determined by GC-MS (CI, ammonia gas) and values corrected for H_2O_2/H_2O isotopic composition[a]

H_2O	**H_2O_2**	**Catalyst**	**Acid (mol%)**	**Measured percentages for**					***cis*-diol[b]**	**epoxide[b]**	**T.O.N.**	
				$[M+NH_4]^+$ (m/z 162)			$[M+NH_4]^+$ (m/z 144)		**$\%^{16}O^{18}O$**	**$\%^{18}O$**	***cis*-diol**	**epoxide**
				cis-diol (%)			Epoxide (%)					
				$^{16}O^{16}O$	$^{16}O^{18}O$	$^{18}O^{18}O$	^{16}O	^{18}O				
^{16}O	^{18}O	**2a**	CCl_3CO_2H (1)	51.8	47.7	0.6	83.8	16.2	103.9	71.2	120	55
^{18}O	^{16}O	**2a**	CCl_3CO_2H (1)	10.9	88.0	1.1	64.4	35.6	93.0	37.6	105	52
^{18}O	^{16}O	**2a**	-	15.5	75.4	9.0	80.3	19.7	79.7	20.8	12	18
^{18}O	^{16}O	**2a**	CCl_3CO_2H (25)	11.0	88.0	1.1	68.3	31.7	93.0	33.5	96	50
^{18}O	^{16}O	**2a**[c]	CCl_3CO_2H (1)	9.3	89.8	0.9	63.8	36.2	94.9	38.2	67	58
^{18}O	^{16}O	**2a**[d]	CCl_3CO_2H (1)	31.9	67.5	0.6	77.2	22.8	95	32	427	234
^{18}O	^{16}O	**6**	2,4-dichlorobenzoic acid (1)	13.8	85.0	1.2	87.3	12.7	89.8	13.4	60	24
^{18}O	^{16}O	**6**	2,4-dichlorobenzoic acid (25)	10.5	88.9	0.6	89.6	10.4	93.9	11.0	109	40
^{18}O	^{16}O	**7**	2,6-dichlorobenzoic acid (3)	11.5	87.8	0.7	82.3	17.6	92.8	18.6	115	12
^{18}O	^{16}O	**9**	4-hydroxybenzoic acid (1)	16.3	81.8	2.0	89.0	11.0	86.4	11.6	20	37
^{18}O	^{16}O	**8**	2-hydroxybenzoic acid (1)	22.6	75.5	1.9	97.1	2.9	81.6	3.1	23	50

a) ^{18}O-labelling studies where performed on cyclooctene on $^1/_{20}{}^{th}$ scale of the standard conditions, with the adjustment that a 2% H_2O_2 solution was used and the peroxide was added batch wise in four portions every 15 min (i.e. at the same rate and amount of H_2O_2 addition under typical reaction conditions). ^{18}Oxygen incorporation was determined by GC-MS (CI) after 60 min reaction time. b) values +/-5%. c) *cis*-heptene as substrate. d) with 20 % $H_2O_{2(aq)}$ solution.

Reactivity and potential involvement of peracids

Burgess,[2] Stack,[3] Que,[4] and co-workers have demonstrated the use of Mn- and Fe-complexes in combination with peracids (either prepared *in situ* from the corresponding acid and H_2O_2 or preformed) in the epoxidation of alkenes. In the present system the combination of H_2O_2 and carboxylic acids, raises the possibility of the involvement of *in situ* formation of peracids.

The oxidation of cyclooctene was performed with both peracetic acid (PAA) and *m*-chloroperbenzoic acid (*m*CPBA) as oxidant (Table S10). Whereas **1** and either acetic acid or 3-chlorobenzoic acid afforded a *cis*-diol/epoxide ratio of ~2:1, with peracetic acid (39% in CH_3CO_2H) or *m*CPBA, almost quantitative epoxidation is observed with formation of only minor amounts of *cis*-diol (~3%, Table S10) and no *trans*-diol.[5] Based on the control experiments performed with peracids (PAA and *m*CPBA) and the lack of activity of Mn(II) and Mn(III) salts with trichloroacetic acid and H_2O_2 (Table S11), it can be excluded that *cis*-dihydroxylation is obtained from the *in situ* formation of peracids. Furthermore, with the alkyl hydroperoxide, tert-butyl-hydroperoxide, as oxidant no significant conversion of cyclooctene is observed.[6]

Table S10 Product distribution following peracid oxidation of cyclooctene

Entry	catalyst (0.1 mol%)	additive (mol%)	conv.	t.o.n.		mass.	oxidant
			(%)	*cis*-diol	epoxide	bal. (%)	
I	**1**	acetic (1)	14	78	36	98	H_2O_2
II	**1**[a,b]	-	97	26	919	97	PAA
III	**3**	-	70	0	668	97	PAA
IV	- [a,c]	-	85	0	838	99	PAA
V	**1**	3-chlorobenzoic (1)	38	253	113	98	H_2O_2
VI	**1**	3-chlorobenzoic (1)	74	6	715	98	mCPBA[d]
VII	**11**	3-chlorobenzoic (1)	81	8	740	94	mCPBA[d]
VIII	**-**	-	91	0	899	99	mCPBA[d]

a) added by syringe pump over 6 h. b) A lag time was observed, see also Murphy et al.[7] b c) no lag time observed. d) added as a 1.3 M solution in acetonitrile.

Table S11 Product distribution following oxidation of cyclooctene catalyzed by **1**, Mn(II) and Mn(III) salts in acetonitrile, in the absence and presence of tmtacn ligand.

Entry	catalyst (mol%)	acid (mol%)	conv.	t.o.n.		mass.
			(%)	*cis*-diol	epoxide	bal. (%)
I	**1** (0.1)	-	3	12	7	99
II	tmtacn (0.11)+$Mn(OAc)_3.2H_2O$ (0.1)	-	1	0	26	101
III	$Mn(OAc)_3.2H_2O$ (0.1)	trichloroacetic (1)	0	0	0	100
IV	$MnSO_4$ (0.1)	trichloroacetic (1)	0	0	0	101
V	$MnSO_4$ (0.2)	trichloroacetic (25)	0	0	0	102
VI	$Mn(ClO_4)_2.6H_2O$	trichloroacetic (25)	3	0	0	97
VII	tmtacn (0.11)+$Mn(ClO_4)_2.6H_2O$ (0.1)	trichloroacetic (1)	52	293	141	91
VIII	tmtacn (0.11)+$Mn(OAc)_3.2H_2O$ (0.1)	trichloroacetic (1)	71	402	204	90
XI	**1** (0.1)	HPF_6 (1)	3	8	19	100
XII	**1** (0.1)	$(Et)_4N.AcO$ (1)	0	0	6	109

FTIR spectroscopy

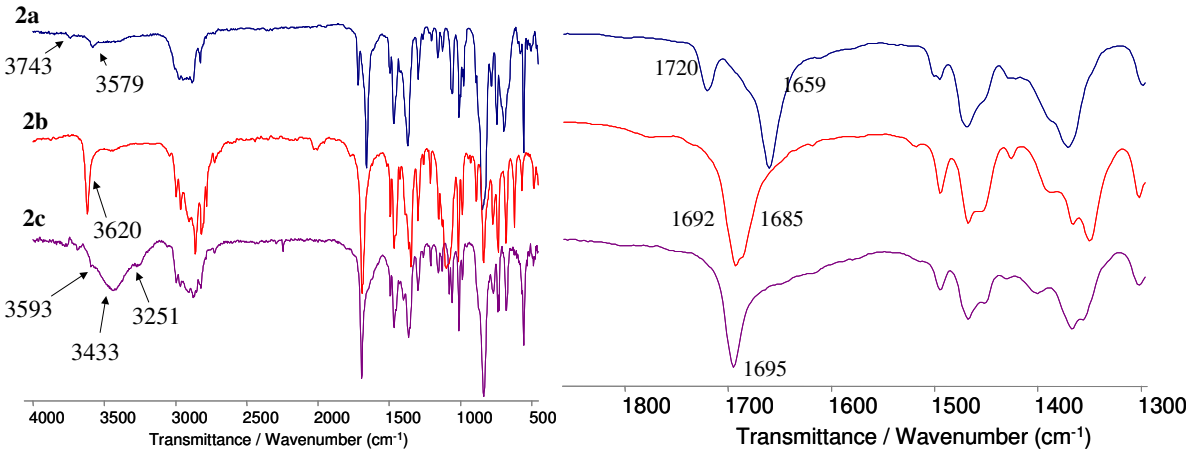

Figure S1 Solid state FTIR spectra (in KBr powder) of **2a**, **2b** and **2c**.

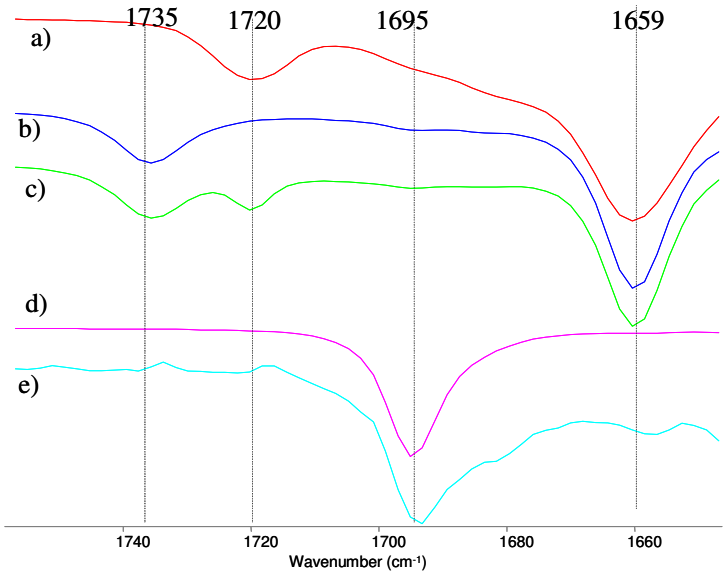

Figure S2 FTIR spectra **2a** a) in KBr powder (solid state), b) in CH_3CN (solvent subtracted), c) in CH_3CN/ 10 mM CCl_3CO_2H (solvent subtracted), **2b** d) in CH_3CN/ 1 M cyclooctene (solvent subtracted) and **2c** e) in CH_3CN/ 1 M cyclooctene (solvent subtracted).

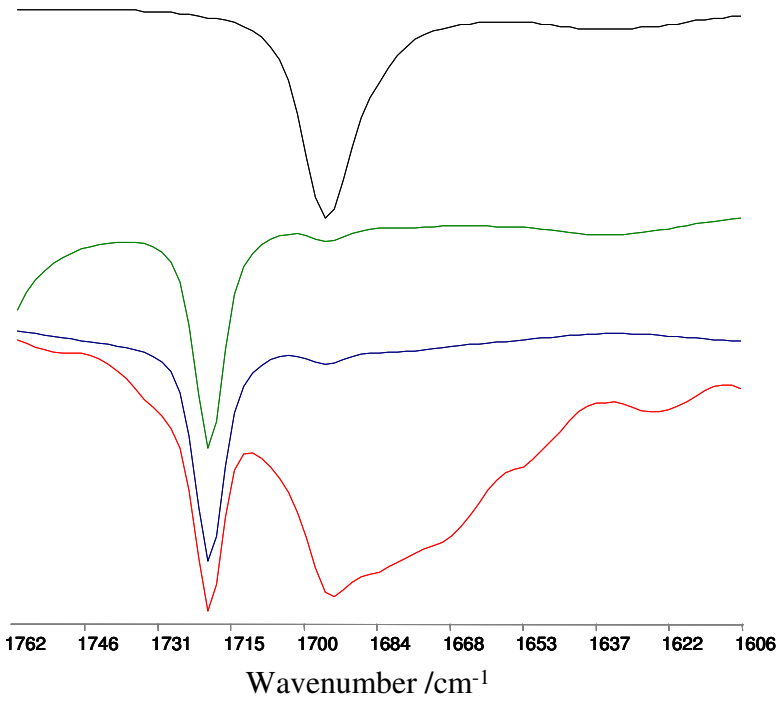

Figure S3 FTIR spectra a) **2b** in CH_3CN (black) b) **2b** in CH_3CN with CCl_3CO_2H (10 mM) (green), c) **2b** in CH_3CN with CCl_3CO_2H (10 mM) and cyclooctene (1 M) (blue) and d) as for (c) except with 5% D_2O (red). (spectra are solvent subtracted).

Cyclic voltammetry and spectroelectrochemistry.

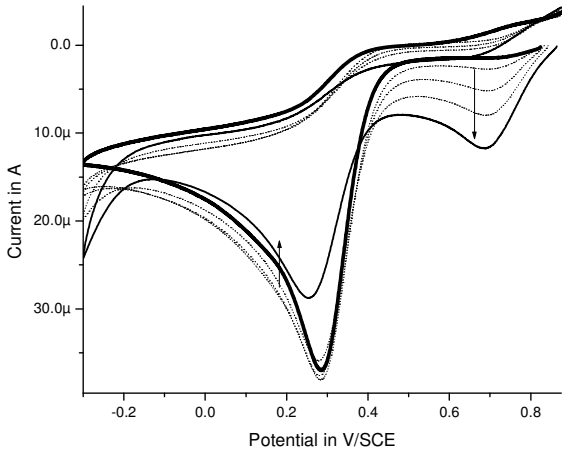

Figure S4 Cyclic Voltammetry of **2a** (1 mM) in CH_3CN/ 0.1 M $TBAPF_6$ vs SCE, in the presence of 1 mM (thick line), 5, 10, 50 mM (dotted lines) and 250 mM (thin line) CCl_3CO_2H. Initial scan direction is negative beginning at the open circuit potential.

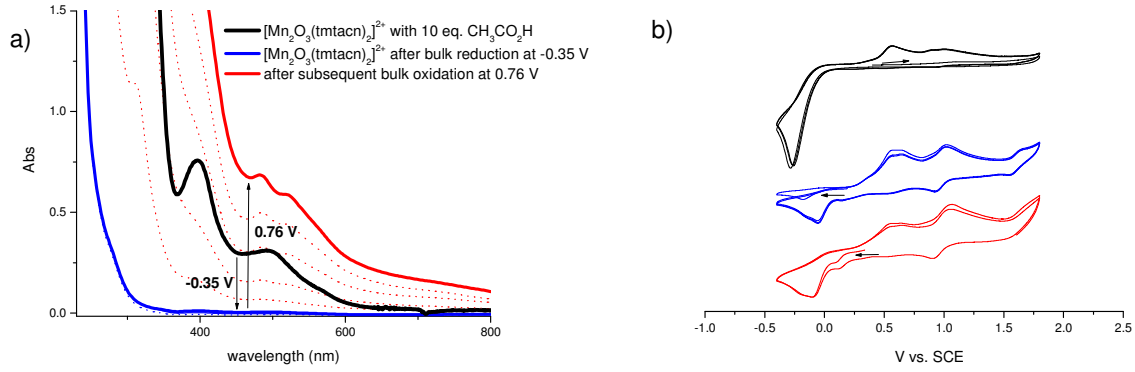

Figure S5 a) UV.Vis spectra of **1** (1 mM) with CH_3CO_2H (10 mM) in CH_3CN/0.1 M KPF_6 (Left: UV.Vis spectrum, right: expansion of visible region) before (black line) and after (blue line) bulk reduction at -0.35 V, and after bulk reoxidation at 0.76 V (red line). b) Cyclic voltammetry of **1** (1 mM) in CH_3CN (0.1 M $TBAPF_6$) a) with CH_3CO_2H (10 mM) 0.1 V s^{-1} in CH_3CN/0.1 M KPF_6, before (black line) and after bulk reduction at –0.35 V (blue line) after reoxidation at 0.76 V (red line) initial scan direction anodic from open circuit potential.

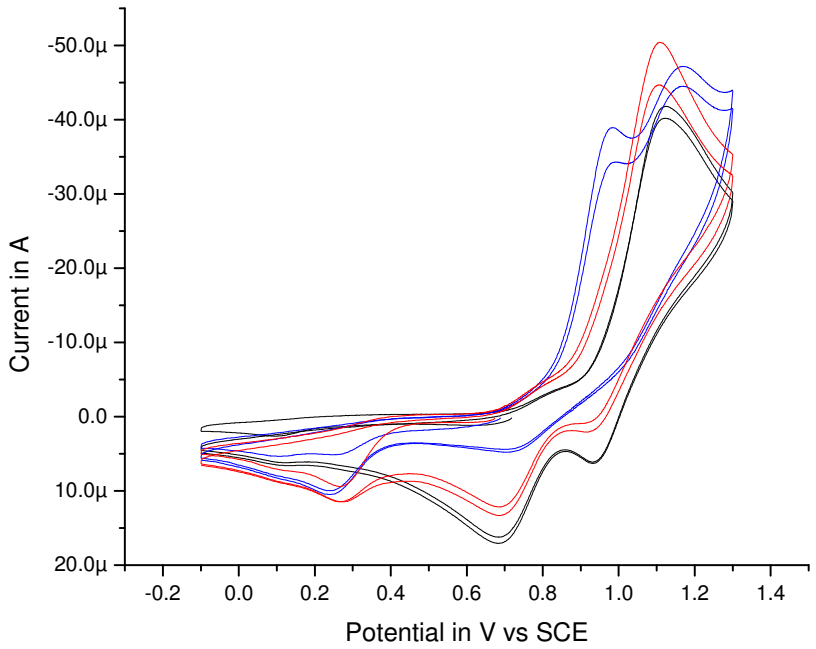

Figure S6 **2b** (1 mM) with CCl_3CO_2H (10 mM), cyclooctene (1 M) and 1,2-dichlorobenzene in 0.1M $TBAPF_6/CH_3CN$: prior to (black) and after (t ~ 30 s, blue) addition of H_2O_2 (50 equiv. w.r.t. **2b**), and 20 min after addition of H_2O_2 (red).

UV.Vis and ^{1}H NMR spectroscopy

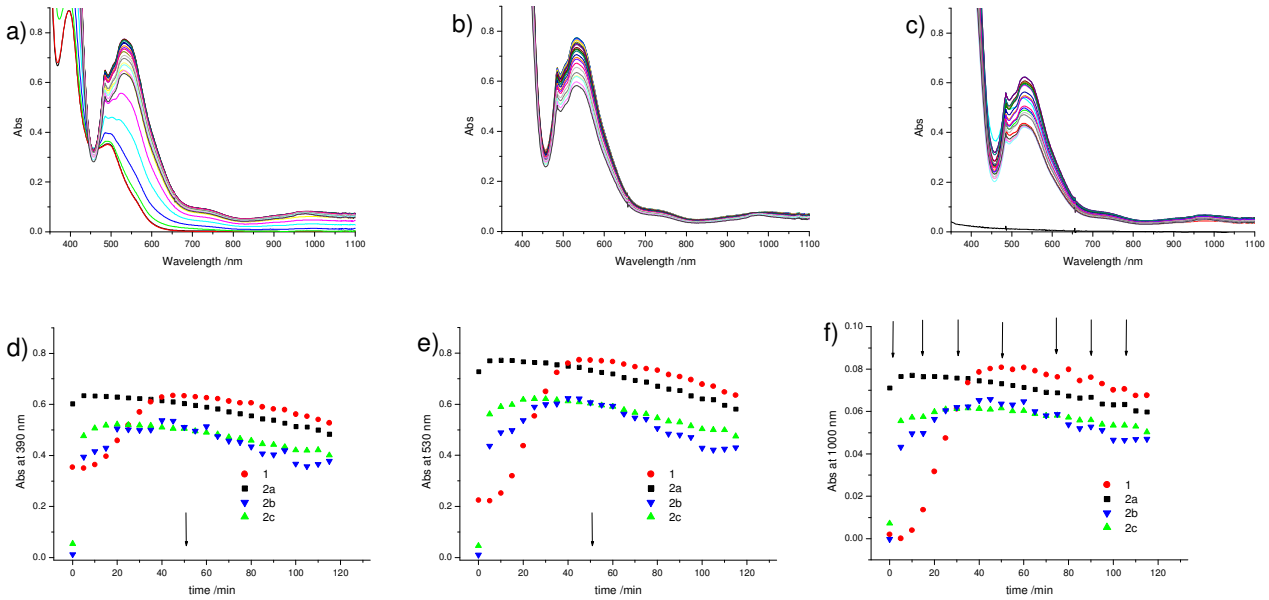

Figure S7 Changes observed in the UV.Vis spectrum of the reaction mixture during the oxidation of cyclooctene (1 M) by H_2O_2 (added batch-wise at a rate of 55 equiv w.r.t catalyst every 15 min) catalyzed by a) **1** (1.26 mM), b) **2a** (1.25 mM) and c) **2b** (1.32 mM) at 20 ^oC with CCl_3CO_2H (10 mM). Changes in absorption observed during catalysis with **1**, **2a**, **2b**, and **2c** (1.25 mM) with CCl_3CO_2H (10 mM) at d) 390, e) 530 and f) 1000 nm. The points of H_2O_2 batch addition indicated by black arrows in graph f.

b)

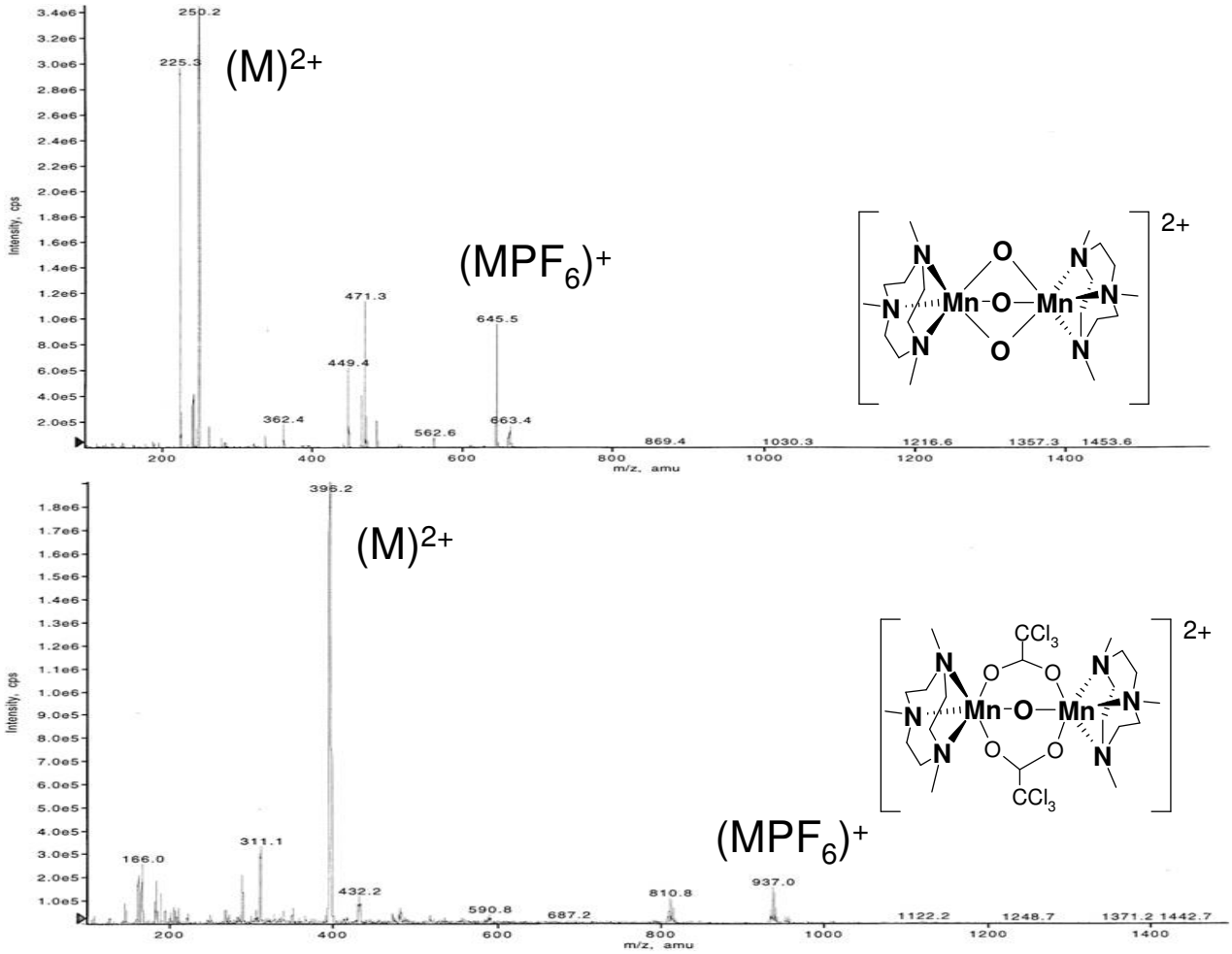

Figure S8 ESI-MS spectra of mixture of **1** (1 mM)/CCl_3CO_2H (10 mM)/cyclooctene after 0 min (upper) and 30 min (lower) at 20 ^{0}C, in CH_3CN.

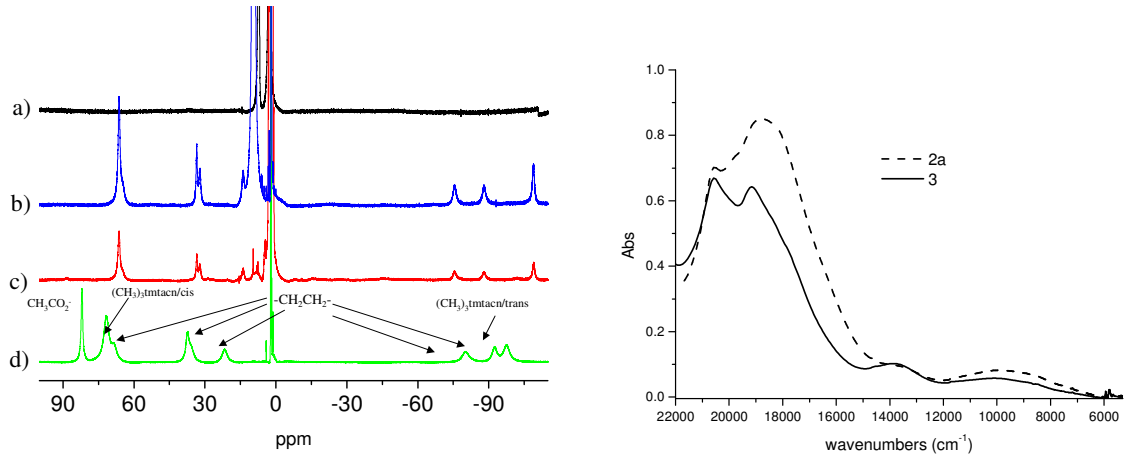

Figure S9 Left: ^{1}H NMR (400 MHz, CD_3CN) spectra of a) **1** (20 mM) with CCl_3CO_2H (200 mM), b) **3** (20 mM) with CCl_3CO_2H (200 mM) after 5 h, c) as for (a) except 1 h after addition of H_2O_2 (53 equiv.) in two portions over 1 h and d) **3** (20 mM). Right: Vis-NIR spectrum of **2a** and **3** (1 mM) in CH_3CN.

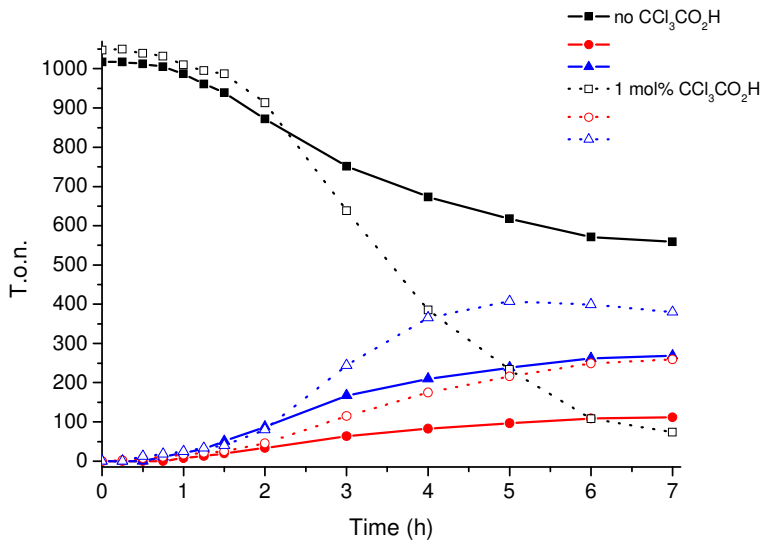

Figure S10 Catalytic oxidation of cyclooctene by **2a** (1 mM) with CCl_3CO_2H (10 mM) (dotted lines) and without CCl_3CO_2H present (solid lines).

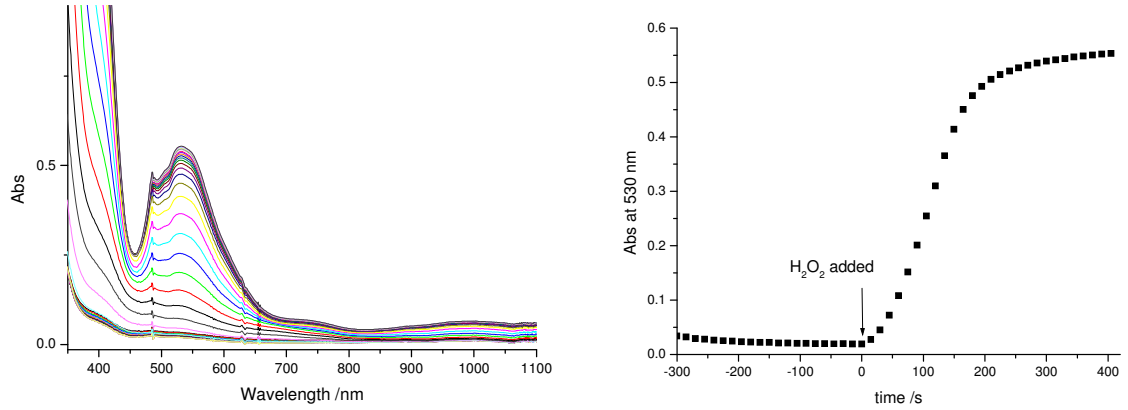

Figure S11 Changes observed in the UV.Vis spectrum of the reaction mixture during the oxidation of cyclooctene (1 M) by H_2O_2 (added batch-wise at a rate of 55 equiv w.r.t **2c** per 15 min) catalyzed by **2c** (1 mM) with CCl_3CO_2H (10 mM) at 20 ^oC Spectra recorded at 30 s intervals.

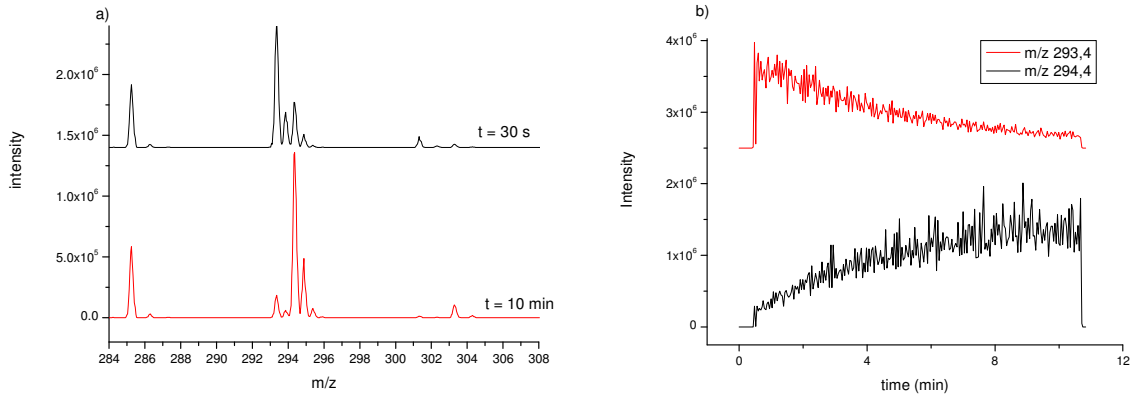

Figure S12 a) ESI-MS spectrum of **3** (1 mM) in CH_3CO_2H (10 mM) with $H_2{}^{18}O/CH_3CN$ 1:9 v/v, at t= 30 s and t = 10 min. b) Time dependence of intensity at 293.4 and 294.4 m/z (traces offset for clarity).

EPR spectroscopy

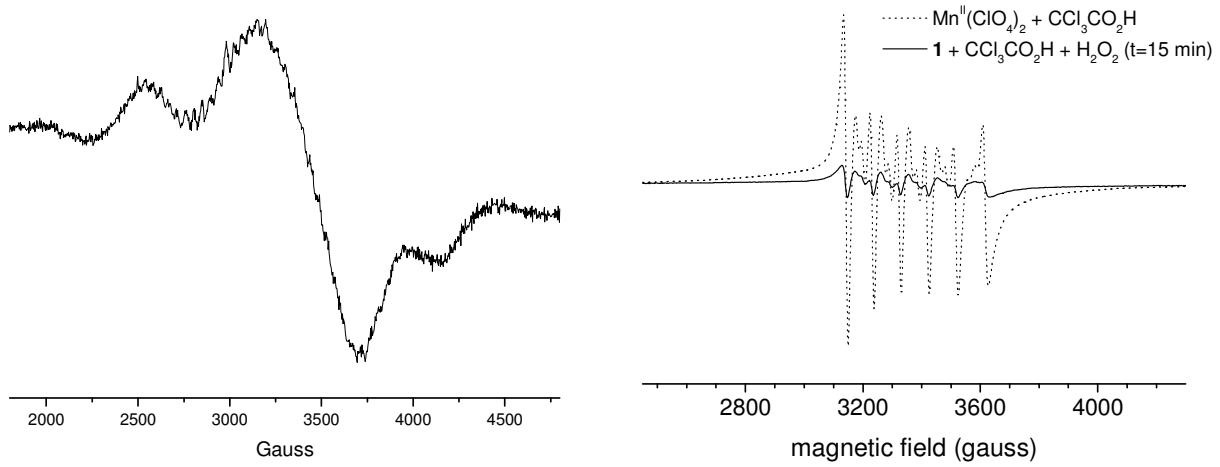

Figure S13 X-band EPR spectrum of left: **2c** in CH_3CN / cyclooctene (1M) [63 mW, 9.466 GHz, 5 dB attentuation] and right: **1** (solid line, 1 mM in CH_3CN with 250 mM CCl_3CO_2H) 15 min after addition of 50 equiv of H_2O_2 and $Mn^{II}(H_2O)_6(ClO_4)_2$ (dashed line, 2 mM in CH_3CN with 250 mM CCl_3CO_2H). Recording conditions: microwave power, 63 mW; modulation amplitude, 0.1 mT; modulation frequency, 50 kHz; time constant, 81.92 ms; T, 77 K; 9.47 GHz.

(a) (b) (c)

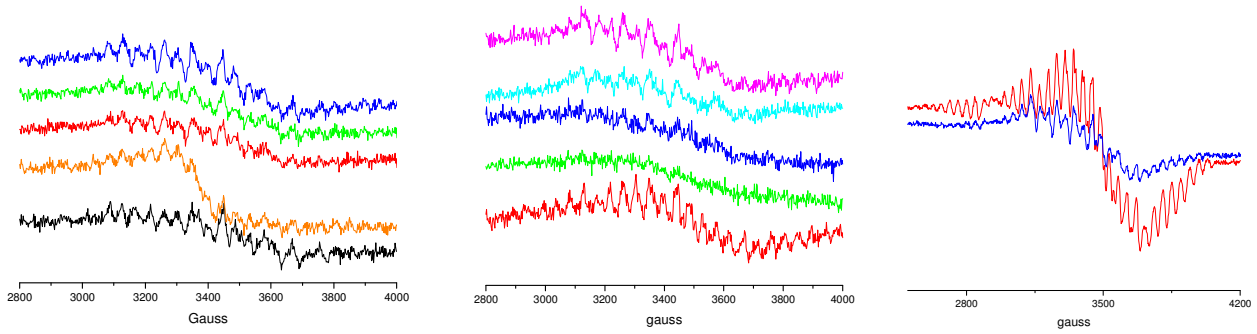

Figure S14 (a) X-Band EPR spectra of **1** 1 mM in CH_3CN with CCl_3CO_2H acid (10 mM) and 1 M cyclooctene: from bottom to top t = 15 (black), 30 (orange), 45 (red), 46 (immediately after H_2O_2 addition) and 60 (blue) min. (b) X-band EPR spectra of **2a** 1 mM in CH_3CN with CCl_3CO_2H acid (10 mM) and 1 M cyclooctene: t = 0 (red), 15 (green), 30 (blue), 45 (cyan) and 60 (pink) min. c) **2b** 1 mM in

CH_3CN with 10 equiv. of CCl_3CO_2H acid during the oxidation of cyclooctene with H_2O_2: t = 0 (red) and 60 (blue) min. Recording conditions: microwave power, 20.1 mW; modulation amplitude, 0.1 mT; modulation frequency, 50 kHz; time constant, 81.92 ms; T, 77 K; 9.47 GHz.

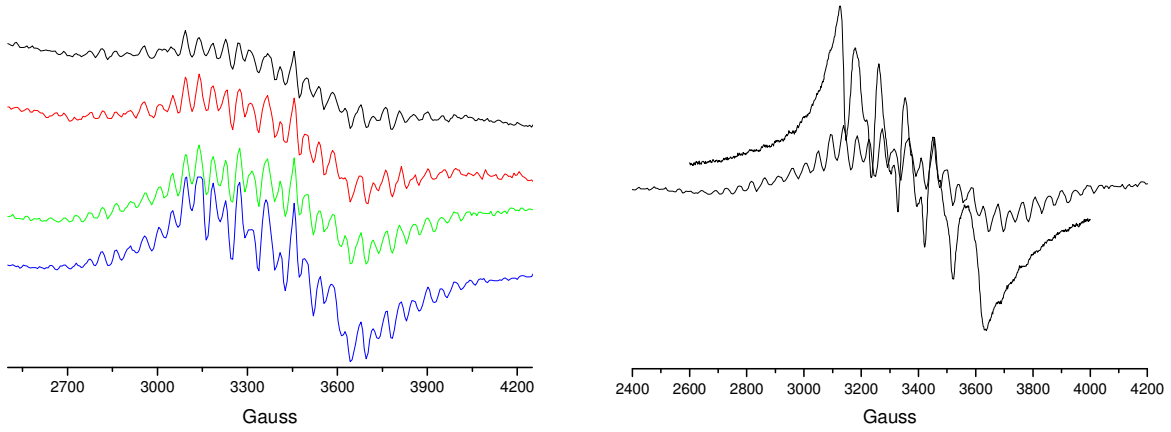

Figure S15 EPR spectrum of **1** (5 mM) with trichloroacetic acid (50 mM) with cyclooctene (1 M) in 1/1 v/v butyronitrile/acetonitrile (batch addition of H_2O_2 every 15 min). Left: Top to bottom at t = 10, 17, 29, 44 min. Right: at t = 29, 150 min, at 20 ^{o}C. Recording conditions: microwave power, 20.1 mW; modulation amplitude, 0.1 mT; modulation frequency, 50 kHz; time constant, 81.92 ms; T, 77 K; 9.47 GHz.

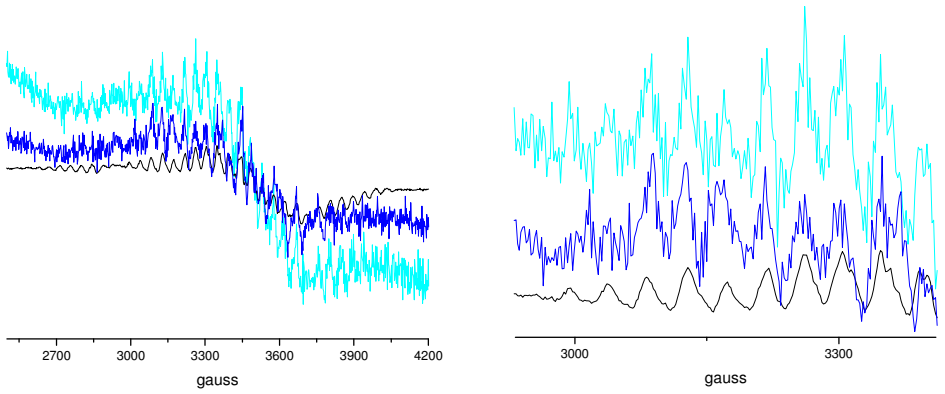

Figure S16 EPR spectra of **2a** (blue) and **2b** (black, 15 times less actual intensity) and **1** (after 15 min of reaction, light blue) 1 mM in CH_3CN with CCl_3CO_2H acid (10 mM) under reaction conditions (10

db/20.1 mW). Recording conditions: microwave power, 20.1 mW; modulation amplitude, 0.1 mT; modulation frequency, 50 kHz; time constant, 81.92 ms; T, 77 K; 9.47 GHz.

ESR spectroscopy for other carboxylate promoted reactions.

Although, the **1**/CCl_3CO_2H catalyzed reaction is the primary focus of the present study, the most effective *cis*-dihydroxylation is observed with **1**/2,6-dichlorobenzoic acid and also with the corresponding bis-carboxylato Mn^{III}_2 complex (**6**), Table 2. For **1**/2,6-dichlorobenzoic acid a much longer lag period (compared to **1**/CCl_3CO_2H) is observed. The evolution of the both the ESI-Mass and EPR specta for this system during catalysis (Figure S17) is remarkably similar to that observed for **1**/CCl_3CO_2H. Nevertheless, distinct differences both in the intensity of the signal corresponding to a $Mn^{II}_2(\mu\text{-}O_2H_3)$ species (akin to **2c**) and the duration over which this signal persists after reaching a steady state concentration at 45 min. For **1**/2,6-dichlorobenzoic acid (1 mol% 2,6-dichlorobenzoic, cyclooctene, 20 ^oC), the formation of **7** $[Mn^{III}_2(\mu\text{-}O)(\mu\text{-}2,6\text{-diCl-benzoate})_2(tmtacn)_2]^{2+}$ (**7**$^{2+}$ m/z 423) from **1** is observed. However, the conversion to **7** was incomplete at 60 min, in agreement with the longer lag period observed during catalysis (by UV/Vis spectroscopy and initiation of cyclooctene oxidation, vide supra). Notably, $[Mn^{II}_2(\mu\text{-}O_2H_3)(2,6\text{-diCl-benzoate})_2(tmtacn)_2]^{2+}$ (m/z 865) and $[Mn^{II}_2(\mu\text{-}2,6\text{-diCl-benzoate})_3(tmtacn)_2]^{+}$ (m/z 1019) ions are observed after 30 min, well before both the onset of catalytic activity and the formation of **7** are observed.

Overall it is apparent that although the formation of Mn^{II}_2 and Mn^{III}_2 bis-μ-carboxylato species occurs at least within 30 min of initiation of addition of H_2O_2 to the reaction mixture, the initiation of catalytic activity is observed only when the Mn^{III}_2 biscarboxylato complexes, e.g. **2a**, **7** etc., form.

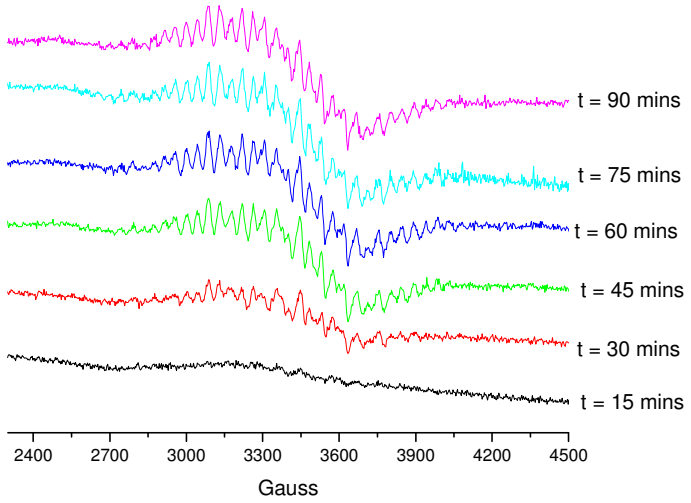

Figure S17 EPR spectra of **1** 1 mM in CH_3CN with 30 equiv. of 2,6-dichlorobenzoic acid under reaction conditions. Recording conditions: microwave power, 20.1 mW; modulation amplitude, 0.1 mT; modulation frequency, 50 kHz; time constant, 81.92 ms; T, 77 K; 9.47 GHz.

---

(1) de Boer, J. W.; Browne, W. R.; Brinksma, J.; Meetsma, A.; Alsters, P.; Hage, R.; Feringa, B.L. *J. Am. Chem. Soc.*, **2005**, *127*, 7990-7991.

(2) Lane, B. S.; Vogt, M.; DeRose, V. J.; Burgess, K. *J. Am Chem. Soc.* **2002**, *124*, 11946-11954.

(3) (a) Dubois, G.; Murphy, A.; Stack, T. D. P. *Org. Lett.*, **2003**, *5*, 2469-2472. (b) Murphy, A.; Pace, A.; Stack, T. D. P. *Org. Lett.* **2004**, *6*, 3119-3122.

(4) (a) Fujita, M.; Costas, M.; Que, Jr., L. *J. Am. Chem. Soc.* **2003**, *125*, 9912-9913. (b) Chen, K.; Costas, M.; Kim, J.; Tipton, A. K.; Que, Jr., L. *J. Am. Chem. Soc.* **2002**, *124*, 3026-3035. (c) Ryu, J. Y.; Kim, J.; Costas, M.; Chen, K.; Nam, W.; Que, Jr., L. *Chem. Comm.* **2002**, 1288-1289. (d) Mas-Balleste, R.; Costas, M.; van den Berg, T.; Que Jr., L. *Chem. Eur. J.* **2006**, *12*, 7489-7500. (e) Oldenburg, P. D.; Que Jr., L;, *Catalysis Today*, **2006**, *117*, 15-21.

(5) Commercially available PAA used (Fluka) consists of 39% peracetic acid in acetic acid (45%) and contains up to 6% of H_2O_2. The formation of *cis*-diol can be attributed to the presence of H_2O_2 (up to 6%) in commercially available PAA and, hence, allows for the formation of **3**.

(6) The complex **2a** was employed in this reaction as tBuOOH is not effective in reducing **1** under catalytic conditions.

(7) Murphy, A.; Pace, A.; Stack, T. D. P. *Org. Lett.* **2004**, *6*, 3119-3122.